Experimental Investigation of CCFL in Pressurizer Surge Line with Air-Water

ZW Wang, WX Tian, JT Yu, DL Zhang, G H Su, SZ Qiu, RH Chen
School of Nuclear Science and Technology, Xi'an Jiao Tong University
28 Xianning West Road, Xi'an 710049, China
wxtian@mail.xjtu.edu.cn; wangzw79@126.com; dlzhang@mail.xjtu.edu.cn

B Dong
State Nuclear Power Software Development Center, Beijing, 102206, China
dongbo@snptc.com.cn

ABSTRACT

For the passive AP600/AP1000 plant, the first three stages of ADS (automatic depressurization system) valves are attached to the top of pressurizer. The existence of these valves make liquid flow into and out of the pressurizer an important part of the dynamics during a small break loss-of-coolant accident. After the fourth stage ADS is opened, draining of pressurizer water takes place. Steam generated in a reactor core and water condensed in a pressurizer form a Counter Current Flow (CCF) in the pressurizer surge line. The counter current flow limitation may be taking place at certain flow condition in the surge line and the draining of water from pressurizer is restrained. So the investigation of CCFL is very important for the accurate prediction of coolant inventory and water lever in reactor pressure vessel (RPV).

To investigate the counter current flow phenomenon in the surge line of AP1000, CCFL in pressurizer surge line test loop with a scaling ratio of 1:5 is established and visualization experiments are conducted with air-water working fluid. The experiment is conducted at atmospheric pressure and room temperature with dimensional water level from 0.137 to 0.821 in the pressurizer simulator. The counter current flow processes are recorded by high speed camera and analyzed in detail.

CCFL data at different water levels in the pressurizer simulator is obtained and compared with existing test data. Obvious difference is found between this present CCFL experimental data and available data in public literatures. This discrepancy may be caused by the differences in fluids physical properties, surge line geometry and boundary conditions. The CCFL data can be well normalized by the Wallis parameter and the Kutateladze parameter respectively. The influence of water level in the pressurizer simulator is small but should not be neglected.

KEYWORDS
CCFL, surge line, water level, flooding

1. INTRODUCTION

Counter current two phase flow and flooding phenomena in light water reactor systems are being investigated experimentally and analytically to improve reactor safety of current and future reactors. Interest in flooding has recently increased because Counter Current Flow Limitation (CCFL) in the AP600 pressurizer surge line can affect the vessel refill rate following a small break LOCA and because analysis of hypothetical severe accidents with the current flooding models in reactor safety codes shows that these models represent the largest uncertainty in analysis of steam generator tube creep rupture.

During a hypothetical station blackout without auxiliary feed water recovery, should the hot leg become voided, the pressurizer liquid will drain to the hot leg and flooding may occur in the surge line[1]. Also flooding in the pressurizer surge line of future Pressurized Water Reactors (PWR) with passive safety systems is an important phenomenon in determining the actuation of the Emergency Core Cooling System (ECCS) [2]. Prediction of CCFL in the pressurizer surge line is difficult due to the complex geometry of the surge line. Fig. 1 is a schematic of the APEX surge line, which is quite similar to AP600. The configuration is one of the typical PWR surge lines whose spiral configuration relieves thermal stress.

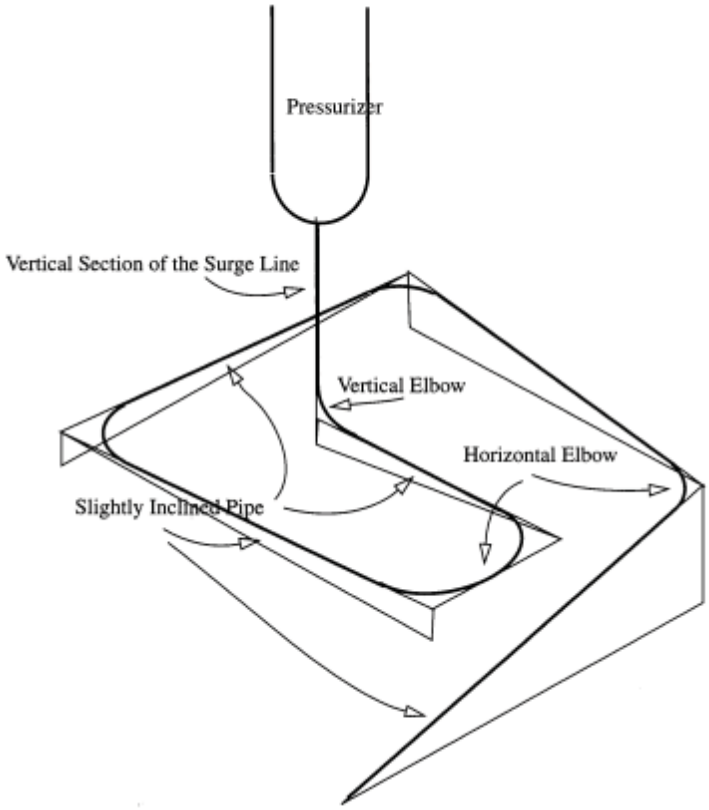

Figure 1. Schematics of OSU pressurizer surge line. [2]

Flooding is the situation in which the flow of a fluid in one direction is large enough to inhibit, partially or completely, the flow of a second fluid in the opposite direction and possibly cause a transition to unstable or co-current flow. Typically, a gas is flowing upward and a liquid is draining downward. This process -considered to be the development of the CCFL phenomenon – can happen in pressurizer surge line. The flow limitation is referred to as Counter-Current Flow Limitation (CCFL) and is experienced under a number of reactor conditions. Flooding can prevent sufficient coolant flow into the reactor core or other reactor components. Counter-current flows of water and steam are of great importance in the field of safety analysis of nuclear reactors ([1],[2],[3],[4]). CCFL can occur in the AP600 pressurizer surge line during reflux condensation [4], SB-LOCA, hypothetical station blackout without auxiliary feed water recovery [1] and Mode 5 Cold Shutdown without Residual Heat Removal (RHR) system [3].

Counter-current flow limitation in a scale-down model of a PWR surge line, which contains a vertical pipe and an inclined pipe with several elbows, was studied by measuring the relationship between the

water and gas flow rates in the surge line. The relationship was referred to as CCFL characteristics. The CCFL took place at three locations in the experiments, that was, at the junction between the vertical pipe and the bottom of the pressurizer, in the inclined pipe and at the junction between the inclined pipe and the hot leg. The CCFL characteristics strongly depended on the location of CCFL. This implied that the CCFL at the junction between the vertical pipe and the bottom of the pressurizer plays an important role in the actual surge line under the reflux condensation [4].That is, the vertical CCFL controls the pressurizer liquid drain rate ([2], [4]). In the present study, the effects of water level in the pressurizer simulator on CCFL characteristics were investigated by controlling the experiments. The flow rate of water entering into PRV simulator was measured to obtain the CCFL characteristics. Flow patterns in the surge line were observed by using a high-speed video camera and the pressure difference between the pressurizer simulator and the vertical section of the surge line model was measured to understand relations between CCFL characteristics and flow patterns in the surge line. Furthermore the CCFL data normalized by the Wallis parameter and the Kutateladze parameter were investigated respectively. The goals of this work are to obtain two-phase counter-current flow pattern and a better understanding of the phenomena in the surge line.

2. EXPERIMENT APPARATUS AND PROCEDURES

A schematic diagram of the experiment apparatus is shown in Fig. 2. The main components consists of the test section (the surge line model), the reactor pressure vessel (PRV) simulator, the pressurizer simulator located at the upper end of the test section, the air supply system, the water supply system and the air and water measuring system. The horizontal tube is used to connect the PRV simulator and the lower end of the test section. The test section is modeled after AP1000 pressurizer surge line with a scaling ratio of 1:5. The surge line has a vertical pipe section connected to a slightly inclined horizontal pipe connected via a vertical elbow. It is then connected to another slightly inclined straight pipe via a horizontal elbow. Due to the complicated counter current two-phase flow behavior in the surge line, it was necessary and possible to visualize the test section ,the horizontal tube, the upper pressurizer simulator and the lower PRV simulator (shown in Fig. 3), which are all made of acrylic resin for the observation of flow pattern. The flow behavior is recorded by a high-speed video camera at the frequencies of 60 Hz and a shutter speed of 1/300 s.

To keep the tube end condition between the surge line and the pressurizer was the same as the prototype, the Pressurizer simulator was modeled after the AP1000 Pressurizer with a scaling ratio of 1:5. That is:

$$[\frac{D_{surge}}{D_{pressurizer}}]_R = 1 \quad (1)$$

Also the horizontal tube is modeled after the hot leg with the same ratio. The water levels in both separators are determined by the measurement of the differential pressure between the top and the bottom of the vessels with differential pressure transducers. A mass flow meter is used to measure the injected water mass flow rate. The injected air mass flow rate was measured and controlled using a vortex flow meter. The down-flowing water mass flow rate (discharge flow) is determined by calculating the increase of water level of the RPV simulator. The temperatures both of the air and water are measured by thermocouples. The differential pressure between the Pressurizer simulator and the vertical section of the surge line is measured by a differential pressure transducer. As well as for the differential pressure in the inclined section of the surge line and the T-junction between the surge line and the hot leg simulator. The signals of the pressure sensors, the water levels inside both simulators, injection mass flow rates and both the air and water temperatures are transmitted to a personal computer via a data acquisition system.

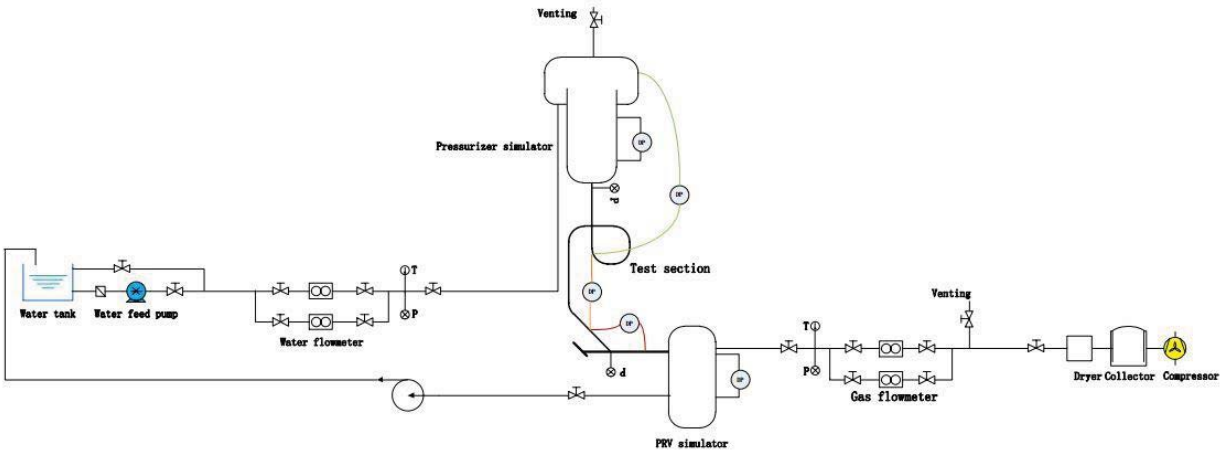

Figure 2. Schematic diagram of the experimental apparatus.

The air-water experiment are performed under the atmospheric pressure. To obtain an initial holdup of water in the pressurizer simulator, a continuous low flow rate of air is first supplied into the lower PRV simulator and flowed through the test section to the upper pressurizer simulator, from which it is released to the atmosphere. The water from the feed water pump is injected into the upper pressurizer simulator until the water level reaches a specified level. After that, the flow rate of air is regulated at a specified mass flow rate W_g, and the flow rate of water injected into the separator tank is also regulated so that the water level h_U in the upper pressurizer simulator might be kept at the specified level. The water level in the pressurizer simulator is kept constant during an experiment. After that, the mass flow rate of falling water $W_{l,d}$ is calculated with the rising velocity of water level in the PRV simulator under a constant W_g of air. After $W_{l,d}$ is measured for a specified W_g, the water in the pressurizer simulator is drained. The procedure mentioned above is repeated to obtain $W_{l,d}$ by a stepwise increase of the air flow rate with a small increment (2-10g/s). The experiments are carried on until the point of zero liquid penetration appears, when the down-flowing water mass flow rate is equal to zero. An overview of the experimental conditions analyzed in this work is given in Table 1.

Table 1

Parameter	Unit	Point	Range
System pressure	MPa	1	0.1
Fluid temperature	℃	-	18-30
Dimensional water level	-	6	0.137-0.821
Air flow rate	kg/s	-	0.01-0.08
Number of plateaux	-	-	22-26
Difference between two plateaux	g/s	-	2-10

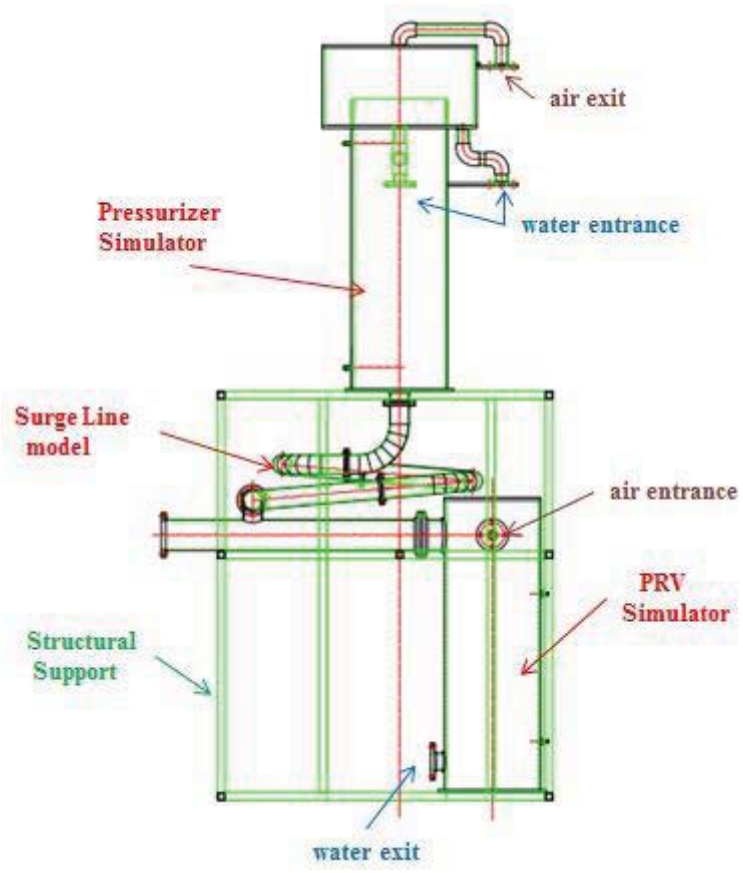

Figure 3. Schematic view of the surge line model test section for visualization.

3. RESULTS AND DISCUSSION

3.1 . FLOW BEHAVIOR OBSERVED IN THE VERTICAL SECTION OF THE SURGE LINE MODEL

3.1.1. FLOW BEHAVIOR AT LOW AIR FLOW RATE

Fig. 4 shows the measured data of the water levels inside both of the PRV simulator and pressurizer simulator, the pressure difference between the pressurizer simulator and the vertical section of surge line model. During this flooding experiment performed at a low air flow rate, water level in the pressurizer simulator keeps at a constant dimensionless value (h/H=0.456) with a variation of maximum $\pm$2.9%. From the slopes of the curve of the water level in the PRV simulator shown in Fig. 4, the water level increases quickly with a low air flow rate. It is also found that the pressure difference between the vertical section of surge line model begins to present high fluctuations. The flow behavior can be described from the high-speed camera images shown in Fig. 5. It should be noticed that two flooding phenomena based on different mechanisms happens in the vertical section and vertical elbow of the surge line model. The one is that the downward annular flow transforms into upward liquid film flow happened in the vertical section of the surge line model, the other is counter-current entrainment phenomenon happened in the vertical elbow of the surge line model. First, The draining of liquid in the pressurizer simulator takes place, and downward annular flow occurs (Fig. 5(a)). Then, the downward annular flow is transformed

into upper liquid film flow(Fig. 5(b)). The partially reversed flow is clearly visible at this section. After that, the inclined two-phase interface plane begin to take form in the vertical elbow of the surge line under the action of force from the gas phase. Then the liquid droplet generated from the inclined two-phase interface plane colliding with the considerable draining water was entrained to the end of the vertical elbow (Fig. 5(c)). Eventually the entrained water flow back with the draining water in the direction of main liquid flow (Fig. 5(d)).

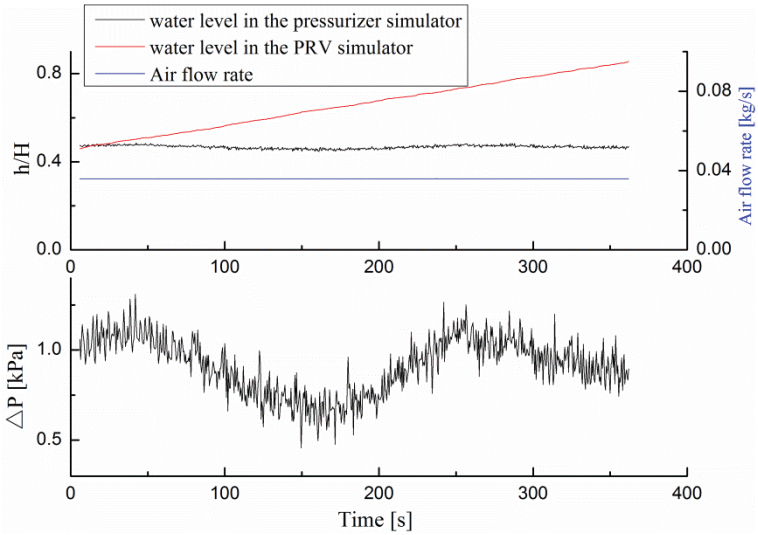

Figure 4. Variation of water level in the PRV simulator (top diagram, red curve) and in the pressurizer simulator (top diagram, black curve), of the air flow rate (top diagram, blue curve), of the pressure difference between the pressurizer simulator and the vertical section of the surge line (bottom diagram, black curve) measured at a low air mass flow rate.

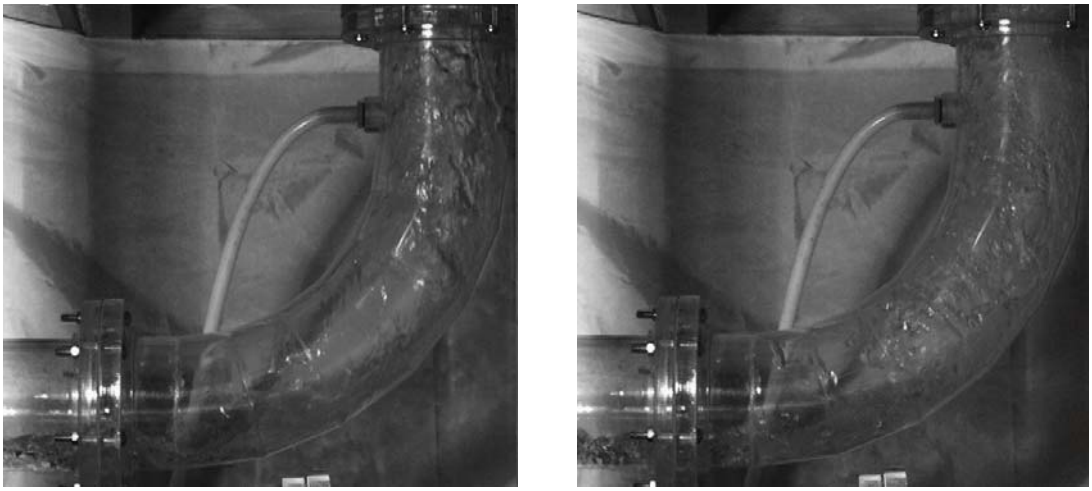

(a) (b)

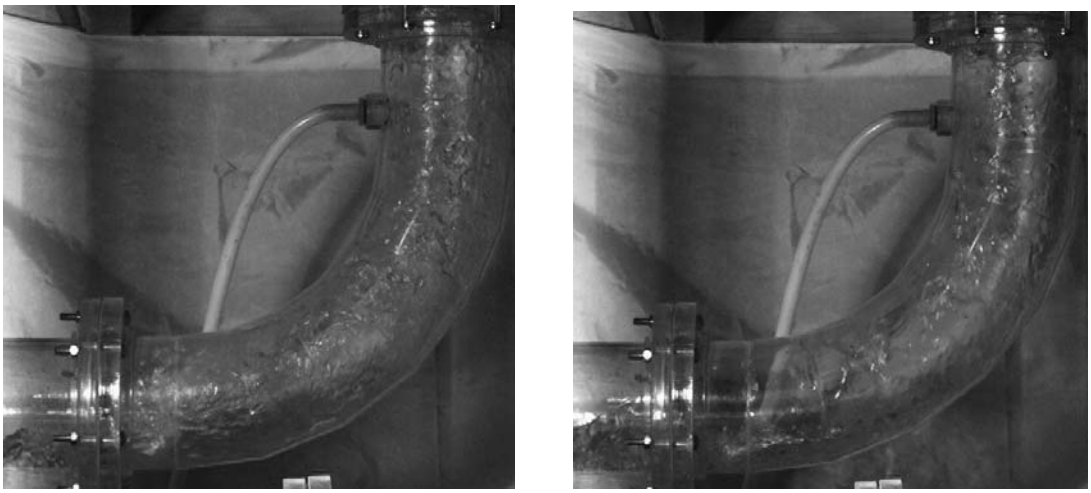

(c) (d)

Figure 5. Flow behavior during the counter-current flow of air and water at low air flow rate (h/H=0.456).

3.1.2. FLOW BEHAVIOR AT HIGH AIR FLOW RATE

Fig. 6 shows the same data like Fig. 4, but with a higher air flow rate. From the slopes of the curve of the water level in the PRV simulator shown in Fig. 6, the water level increases slowly with a high air flow rate. It is also found that the pressure difference between the vertical section of surge line model begins to present high fluctuations. The flow behavior can be described from the high-speed camera images shown in Fig. 7.

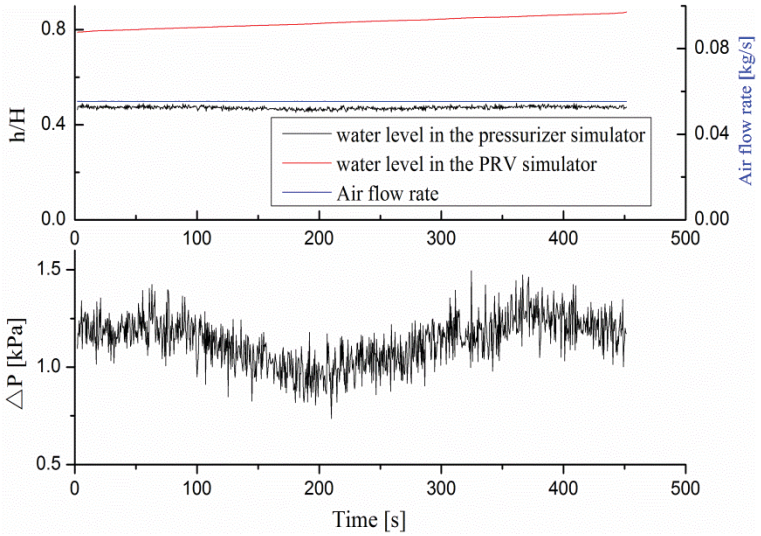

Figure 6. Variation of water level in the PRV simulator (top diagram, red curve) and in the pressurizer simulator (top diagram, black curve), of the air flow rate (top diagram, blue curve), of the pressure difference between the pressurizer simulator and the vertical section of the surge line (bottom diagram, black curve) measured at a high air mass flow rate.

As is shown in Fig. 7, the two flooding phenomenon occur at the vertical section and vertical elbow of the surge line under this flow rate of gas phase at the same time. Downward annular flow occurs at the

vertical section, and the inclined two-phase interface plane begin to take form in the vertical elbow of the surge line simultaneously (Fig. 7(a)). Then, the downward annular flow is transformed into upper liquid film flow, and the liquid droplet generated from the inclined two-phase interface plane colliding with the considerable draining water is entrained to the end of the vertical elbow or even to the vertical section (Fig. 7(b)). After that, the draining of liquid in the pressurizer simulator continues to take place (Fig. 7(c) and Fig. 7(a)). Periodically, the flooding and entrainment phenomenon take place at the vertical section and the vertical elbow of the surge line model.

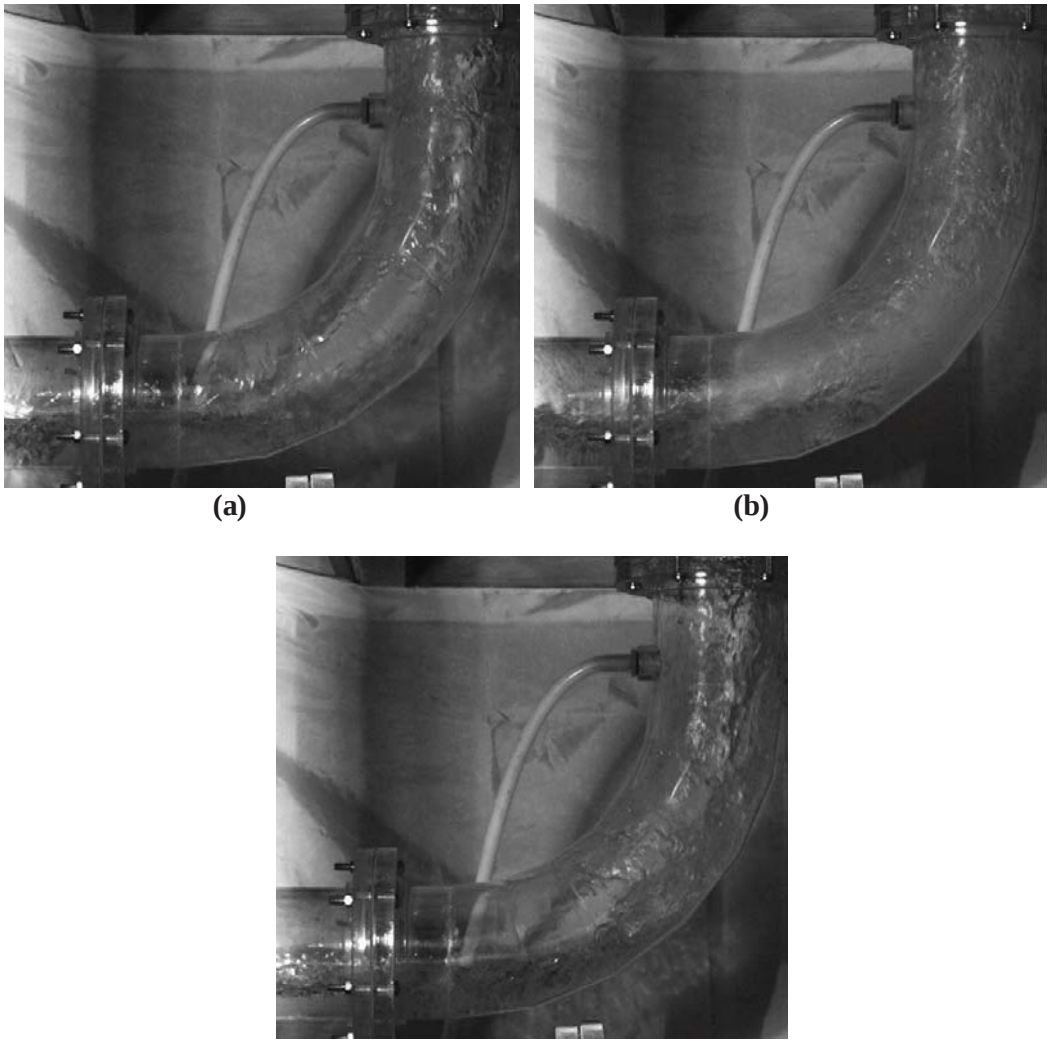

(a) **(b)**

(c)

Figure 7. Flow behavior during the counter-current flow of air and water at high air flow rate (h/H=0.456).

3.2. ANALYSIS OF THE COUNTER-CURRENT FLOW EXPERIMENT

As shown in the previous section, a run can be divided into different regions according to the flow conditions. In each region, the discharged water flow rate ($W_{l,d}$) and air mass flow rate (W_g) are almost constant and can be evaluated, $W_{l,d}$ is determined from the increase of the water level in the RPV simulator. The slope of a linear regression through the measured points is used to calculate the discharge

water flow rate. This method limits the influence on the results of perturbations appearing sometimes in the measured signal due to the highly disturbed flow conditions during CCFL. As an example, the plot of the discharged water flow rate ($W_{l,d}$) versus that of air mass flow rate (W_g) measured in this way is shown in Fig. 8. In this case, the dimensionless water level in the pressurizer simulator is h_U/H=0.456. It can be observed that the discharged water flow rate is high at low air mass flow rate between W_1 and W_2. In this region, flooding takes place only at the vertical section of the surge line model (Flooding-U). As W_g is increased between W_2 and W_3, $W_{l,d}$ begins to decrease, and flooding takes place at the junction of the surge line model and the hot leg model (Flooding-L) and also Flooding-U. As W_g is further increased between W_3 and W_4, flooding takes place at the inclined section of the surge line model(Flooding-S) and also Flooding-U and Flooding-L. In this region, waves are generated in the surge line and move toward the upper junction of the surge line model. As W_g is increased to a critical value, $W_{l,d}$ decreases to zero, at the zero liquid penetration point. The region from the onset of Flooding-U to zero penetration is defined as flooding regime. The data in this region is used to examine available correlation to predict the flooding in a model of PWR surge line as discussed later.

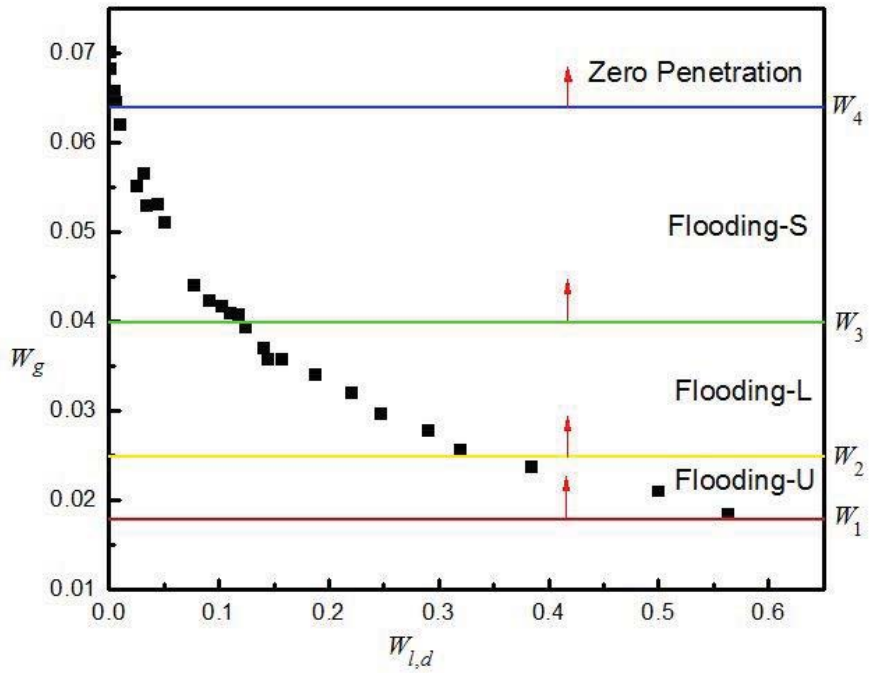

Figure 8. Definition of flooding region (h_U/H=0.456).

3.2.1. FLOODING DATA DESCRIBED BY Kutateladze PARAMETER

Richter [5] and Jayanti et al. [6] suggested that, for prediction of flooding, the Wallis parameter, J^* is appropriate for small diameter pipes, whereas the Kutateladze number [7], is better for large diameter pipes. Vijayan et al [8]. carried out flooding experiments using vertical pipes of D=25, 67 and 99 mm and confirmed that J^* is better for small D(25 mm), whereas Ku^* is better for large D (67 and 99 mm). Furthermore, The Idaho National Engineering Laboratory [9] did an analysis specific to APEX and the AP600 and found that Kutateladze scaling is appropriate when D^* is greater than or equal to 32. That is,

$$D^* = D\sqrt{\frac{g\Delta\rho}{\sigma}} \geq 32 \qquad (2)$$

where D is the tube diameter, and σ is the surface tension. Flooding has been adequately correlated for $D^* \geq 32$, sing the Kutateladze flooding correlation which is defined as follows:

$$\sqrt{Ku_g^*} + m\sqrt{Ku_{l,d}^*} = C \tag{3}$$

The Kutateladze number is defined as:

$$Ku_i^* = j_i[\frac{\rho_i}{[g\sigma(\rho_l - \rho_g)^{0.5}]}]^{0.5} \quad (i = (l,d), g) \tag{4}$$

As seen in equation (3), the flooding condition is independent of tube diameter when $D^* \geq 32$. In this equation the characteristic length is given by a critical wavelength expressed as follows:

$$\lambda = (\frac{\sigma}{g(\rho_l - \rho_g)})^{0.5} \tag{5}$$

3.2.1.1. INFLUENCE OF WATER LEVEL IN THE PRESSURIZER SIMULATOR ON CCFL

The CCFL characteristics measured for various water levels in the Pressurizer simulator shown in Fig. 9 are discussed in this section. Various water levels in the Pressurizer simulator were test. The water level in the PRV simulator is kept increasing during the data collection. So $W_{l,d}$ is calculated from the amount of draining water collected in the PRV simulator. The result shows the lower the air flow rate, the lower and the larger effects on liquid flow rate with increasing water level in the Pressurizer simulator, while the results is opposite at high air flow rate.

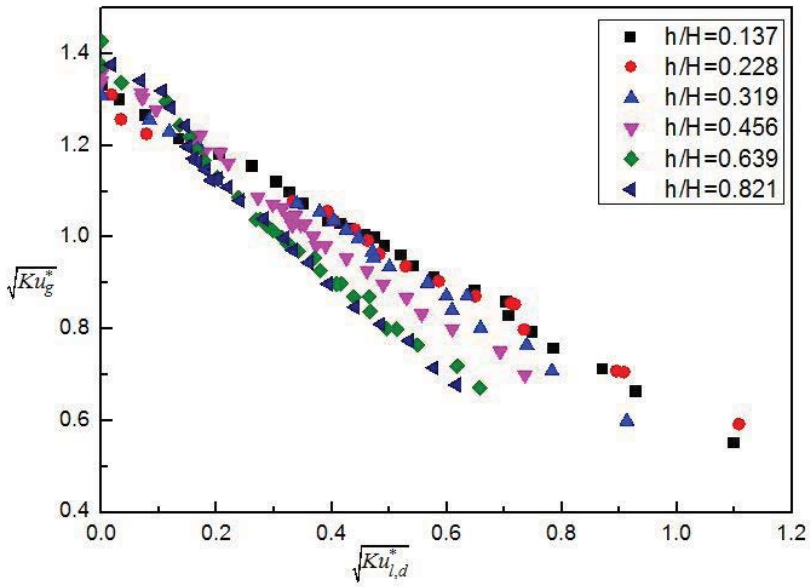

Figure 9. Effects of water level in the Pressurizer simulator on CCFL characteristics (kutateladze parameter).

3.2.1.2. COMPARISON OF THE PRESENT CCFL DATA WITH OTHER STUDY

In the next section, the CCFL data is compared with different experiment data available in the literature. The comparison is based on the evaluation of 6 flooding runs. Since the past research was mostly applied

to pipes, a comparison with the present data could help to identify the influence of the flat geometry of the surge line model on the flooding.

Fig. 10 shows a comparison of the present data with the results of air/water counter-current flows at the junction between the surge line and the pressurizer of a PWR obtained by Taiga et al. [10]. As shown in the figure, the present data deviate significantly from the data of Taiga and Takashi, which cannot be used to predict the CCFL in a surge line model. A close inspection of the figure reveals that the slope of the present CCFL data is slightly lower than that by Taiga and Takashi. The comparison shows that data for flooding at the junction between the surge line and the pressurizer of a PWR, do not predict the CCFL in a model of the surge line satisfactorily. This may be due to the particular geometry of the surge line.

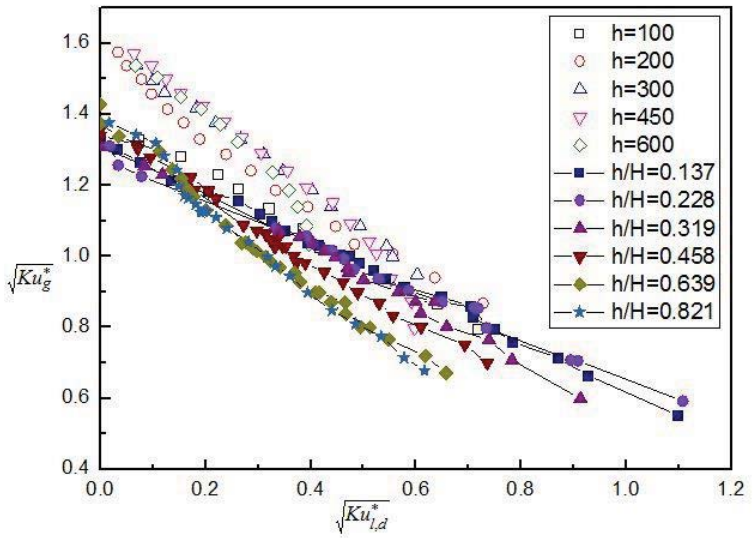

Figure 10. Comparison of the present CCFL data (dash dot line) with data obtained for the junction between the surge line and the pressurizer of a PWR (kutateladze parameter).

3.2.2. FLOODING DATA DESCRIBED BY Wallis PARAMETER

Fig. 11 shows the CCFL characteristics measured for various water levels in the pressurizer simulator, where $J_{l,d}^*$ and J_g^* are the wallis parameter defined by

$$J_k^* = j_k[\frac{\rho_k}{gD(\rho_l - \rho_g)}]^{0.5} \qquad (k = (l,d), g) \tag{6}$$

Where ρ is the density, g the acceleration of gravity and D the pipe diameter.

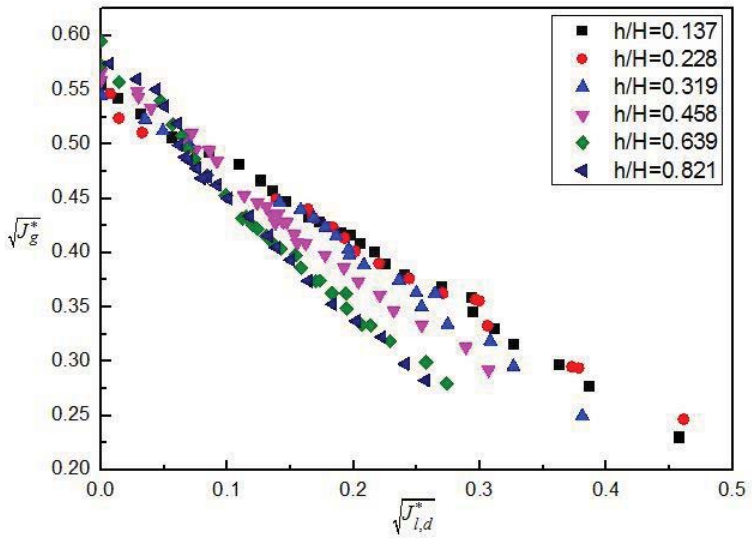

Figure 11. Effects of water level in the Pressurizer simulator on CCFL characteristics (wallis parameter).

Fig. 11 shows the CCFL characteristics measured for various water levels in the pressurizer simulator. This shows that $J_{l,d}^*$ tends to decrease with increasing J_g^*, and gas phase wallis parameter keeps a good linear relationship with liquid phase during a specified water level in the pressurizer simulator. The flow limitation becomes stronger with increasing water level in the pressurizer. Furthermore, just like Fig. 9 shows, the lower the air flow rate, the lower and the larger effects on liquid flow rate with increasing water level in the Pressurizer simulator, while the results is opposite at high air flow rate.

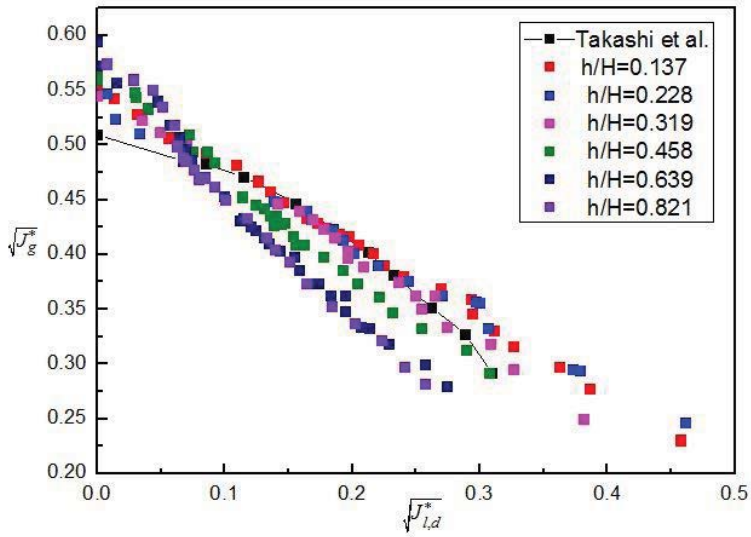

Figure 12. Comparison of the present CCFL data with data obtained for the surge line of a PWR (wallis parameter).

Fig. 12 shows a comparison of the present data with the results of air/water counter-current flows in the surge line of a PWR obtained by Takashi et al. [4]. As shown in the figure, the correlative experiment data are in good agreement with this experiment at dimensionless water level in the pressurizer simulator equal or less than 0.319.

4. CONCLUSIONS

The counter-current flow limitation was investigated experimentally in a surge line model of a PWR. The important counter current flow phenomenon was captured by a high-speed camera in the vertical section of the surge line model during a series of flooding experiments. Air and water at room temperature and atmospheric pressure are supplied, respectively. The flow rate of water entering into the PRV simulator is measured to obtain CCFL characteristics. The main conclusions obtained under the present experimental conditions are as follows.

1) The CCFL characteristics for different water levels in the pressurizer simulator are well correlated using the Kutateladze number as well as the Wallis number. Water level has a slight effect on the CCFL characteristics in the surge line, that is, water penetration into the surge line decreases with the water level, h_U, in the pressurizer simulator increases during low air flow rate. While the results is opposite at high air flow rate.
2) CCFL takes place at three different locations, that is, at the vertical section of the surge line (Flooding-U), at the junction of the surge line model and the hot leg model (Flooding-L) and at the inclined section of the surge line (Flooding-S). CCFL characteristics are governed by the most dominating flow limitation among the three.
3) The experimental data was compared with CCFL data for different pipe and surge line system geometries found in the literature. For this comparison, it is shown that the CCFL characteristics in simple geometry like pipes cannot be used to predict CCFL in the complicated surge line.

NOMENCLATURE

Subscripts

U	the upper pressurizer simulator
l	liquid phase
g	gas phase
l,d	the draining liquid

Superscripts

W	mass flow(kg/s)
D	hydraulic diameter (m)
D_U	water level in the upper pressurizer simulator(m)
$*$	dimensionless quantity
$D*$	dimensionless hydraulic diameter
C	flooding constant
m	flooding coefficient
g	acceleration of gravity(m s^{-2})
j	superficial velocity(m s^{-1})
$J*$	dimensionless volumetric flux
$Ku*$	Kutateladze dimensionless volumetric flux

Greek

ρ	Density(kg/m^{-3})

σ	surface tension(N/m)
λ	a critical wavelength(m)
$\Delta\rho$	density difference, $\rho_l - \rho_g$

ACKNOWLEDGMENTS

The authors are grateful to national science and technology major project of large advanced PWR nuclear power plant in china for their technical guidance and financial support (2011ZX06004-024).

REFERENCES

1. M. Solmos, K. J. Hogan, K. Vierow, "Flooding Experiments and Modeling for Improved Reactor Safety" , *US Japan Two Phase Flow Seminar*, (2008).
2. K. Takeuchi , M.Y. Young, A.F. Gagnon, "Flooding in the pressurizer surge line of AP600 plant and analyses of APEX data", *Nuclear Engineering and Design*, Volume 192, Issue 1, 2 Pages 45 – 58, (1999).
3. Sarah E. Colpo, "Pressurizer Surge Line Counter Current Flow Limitation During AP600 Mode 5 Cold Shutdown", (1999)
4. Takashi Futatsugi, Chihiro Yanagi, Michio Murase, Shigeo Hosokawa, Akio Tomiyama, "Countercurrent Air-Water Flow in a Scale-Down Model of a Pressurizer Surge Line",*Science and Technology of Nuclear Installations*, (2012).
5. H. J. Richter, "Flooding in tubes and annuli," *International Journal of Multiphase Flow*, vol. 7, no. 6, pp. 647–658, (1981).
6. S. Jayanti, A. Tokarz, and G. F. Hewitt, "Theoretical investigation of the diameter effect on flooding in countercurrent flow, " *International Journal of Multiphase Flow*,vol.22,no.2, pp. 307–324, (1996).
7. S. S. Kutateladze, "Elements of the Hydraulics of Gas-Liquid System,"*Fluid Mechanics Soviet Research*, vol. 1, no. 4, pp. 29–50, (1972).
8. M. Vijayan, S. Jayanti, and A. R. Balakrishnan, "Effect of tube diameter on flooding,"*International Journal of Multiphase Flow*, vol. 27, no. 5, pp. 797–816, (2001).
9. Modro, S.M. "Evaluation of Scaled Integral Test Facility Concepts for the AP600", *Idaho National Engineering Laboratory*, SMM-37-91, (1991).
10. Tai ga Doi , Takashi Futatsugi, Michio Murase, Kosuke Hayashi, Shigeo Hosokawa, and Akio Tomiyama, "Countercurrent Flow Limitation at the Junction between the Surge Line and the Pressurizer of a PWR", *Science and Technology of Nuclear Installations*, Volume 2012, Article ID 754724,10 pages, (2012).